JOURNAL OF MATERIALS SCIENCE 26 (1991) 3712–3720

Effect of thermal treatment on various characteristics of undoped and V_2O_5-doped Co_3O_4/TiO_2 catalysts

S. A. HASSAN, M. A. MEKEWI, F. A. SHEBL, S. A. SADEK
Department of Chemistry, Faculty of Science, Ain Shams University, Cairo, Egypt

The thermal treatment of undoped and V_2O_5-doped Co_3O_4/TiO_2 catalysts was studied in the temperature range, 330–600° C both in vacuum and in air. The wide difference in the catalytic behaviour of the two catalysts could be attributed to surface as well as bulk diffusion of the active cobalt oxide particles. Although in both cases the total Co^{3+} ions of various energy states were considered to be the active species for the given reaction, the distribution of various cobalt species, namely Co-t and Co-o, occupying tetrahedral and octahedral sites in the support-defective structure, seemed to be seriously affected by doping with V_2O_5. This dopant was supposed to have two-fold effect: part is incorporated into the surface Co_3O_4 crystallites leading to smaller more mobile particles, easily reducible and more dispersed, and another part diffuses a few atomic layers deeper in the support causing the redistribution of cobalt species. Upon heating, the increased mobility and the increased availability of the support tetrahedral sites may be responsible for the deactivation behaviour. The bulk diffusion enhanced by doping might cause some modification in the porosity characteristics of the titania support.

1. Introduction

The unique electronic behaviour of Co_3O_4 hydrotreating catalyst, as a dual valency system dispersed on the surface of different inert supports, has attracted the attention of several investigators, e.g. [1–7]. The strong metal–support interaction occurred when using a titania surface was of particular interest, e.g. [8–10], where the extent of the interaction was proposed to be dependent on the reducibility of the support [11]. An electron transfer from TiO_2 to the supported metal phase was also reported as accompanying the high-temperature reduction [12, 13]. On the other hand, such a strong interaction could lead to a marked lowering in the hydrogen reducibility of the supported cobalt in several other systems [2, 3, 14]. In general, preparation conditions were found to influence the structural characteristics of this oxidic catalyst system, namely, Co_3O_4/TiO_2, in particular, the cobalt valency, the solid-state diffusion as well as the dispersion and the cluster size of Co_3O_4 [15].

Doping of the unsupported Co_3O_4, especially with V^{5+} ions, was investigated thoroughly [16, 17], which was assumed to be accompanied by some structural changes with the consequence that the reduction of Co_3O_4 to Co O becomes facilitated [18]. In a supported system, where γ-alumina was used, the high-temperature calcination in the presence of a dopant could lead to an increased cobalt–support interaction with the decomposition of Co_3O_4 to Co^{2+} species [19]. However, for the Co_3O_4/TiO_2 catalyst, reports of such doping effects are surprisingly lacking in the literature.

The present study was undertaken to correlate the catalytic activity of thermally treated undoped and V_2O_5-doped Co_3O_4/TiO_2 catalyst systems with both intrinsic factors (e.g. chemical nature and electronic structure) and microstructural factors, aiming to elucidate the nature, dispersion and distribution of active species contributing to the metal–support interaction.

2. Experimental details

2.1. Catalysts

The supported Co_3O_4/TiO_2 catalyst (Co_3O_4 = 3.8 mol % wt/wt) was prepared by impregnation of titania support, outgassed for $1\frac{1}{2}$ h at 110 °C, with the appropriate quantity of cobalt nitrate solution followed by stirring for 12 h. After drying at 110 °C for 24 h, the resulting solid was calcined at 330 °C in atmospheric air for 5 h.

The V_2O_5-doped catalyst (Co_3O_4 = 3.8 mol %, V_2O_5 = 0.6 mol % wt/wt) was prepared by codispersing both Co_3O_4 and V_2O_5 phases on the titania surface by applying the same impregnation technique but with the simultaneous addition of a calculated amount of NH_4VO_3 solution while stirring. The same drying and calcination conditions were used.

The thermal treatment of various catalyst samples was carried out in atmospheric air, i.e. in a flow of dry air, and *in vacuo* using a high-vacuum system, for $\frac{1}{2}$, 1, 2, 4 and 6 h at the required temperature in the range 330–600 °C of industrial interest.

2.2. Catalytic activity

The catalytic activity of various catalyst samples was

0022–2461/91 $03.00 + .12

tested in a simple model reaction, namely, liquid-phase decomposition of H_2O_2 in an alkaline medium (pH = 13.5, using 0.8N KOH), where it is present as perhydroxyl ions, HO_2^- [20]. The kinetics was followed gasometrically through measurement of the volume of oxygen evolved according to

$$2HO_2^- = O_2 + 2OH^- \quad (1)$$

From this volume and half-life period ($t_{\frac{1}{2}}$), the catalytic activity parameter (A), denoting the number of H_2O_2 molecules decomposing per second per gram of catalyst, was calculated applying an equation previously described [21]. Although this reaction is not typical for cobalt catalysts, it was used convincingly here to confirm the role played by the dual valency of active Co_3O_4 phase as functioned by the redox nature of the reaction; moreover, its simplicity was required in correlating the catalytic activity with other structural and textural parameters.

2.3. Dissolution of surface-active species

In a preliminary experiment, 3 ml 2N H_2O_2 solution were placed with 100 mg catalyst sample in the reactor and the catalytic activity (A) was determined as described above. In another experiment, 30 ml dilute HCl (pH = 2) were added to the same catalyst sample, shaken for 5 h, then 3 ml H_2O_2 were added and the activity (A_d) was determined. The degree of deactivation (A_d/A) was found to be entirely proportional to the fraction of the dissolved surface-active species as confirmed by spectrophotometric measurements. The catalyst after filtration and washing several times with doubly distilled water was completely inactive. As the dissolution took place at room temperature, where the diffusion into the solid is very slow, it seemed justifiable to assume that the dissolved species were those located in the surface layers of the catalyst grains. The fraction dissolved, mainly of Co_3O_4, was normalized to 1 g of the supported oxide after correction for TiO_2 and V_2O_5 blanks.

2.4. Surface and bulk excess (active) oxygen

Surface excess oxygen, limited to the cobalt oxide located on the top layers of the catalyst, could be estimated according to the previously published method [22], where 20 ml 0.1N HCl and 1 g KI were added to 0.1 g catalyst sample and the reaction was continued for 3 h at room temperature under a flow of dry nitrogen. The excess oxygen (at %) was estimated in the filtrate using an equation described elsewhere [23] after correction for the effect of free Cl_2, TiO_2 and V_2O_5.

Total excess oxygen could be determined following the same method [23], where 40 ml HCl (1:1) and 10 ml 10% KI solution were added to 0.1 g catalyst sample. While bubbling the purified N_2, the mixture was heated for 1 h in a water bath to effect complete dissolution. The total excess oxygen (at %) and the corresponding number of Co^{3+} ions, surface and bulk, were determined according to an equation given previously [24], assuming the chemisorbed oxygen be in the form of O^{2-} and every O^{2-} ion leads to 2 Co^{3+} ions [23].

2.5. Degree of reducibility and high-temperature chemisorption of H_2 on reduced samples

Following the modified approach of Amelse *et al.* [25], a catalyst sample was reduced for 3 h in a flow of purified H_2 gas at 330 °C and left to cool to room temperature in the same flow. The degree of reducibility (α) was estimated, according to the procedure employed by Gajardo *et al.* [2, 3], as the ratio of reduced oxide/initial oxide, assuming that cobalt oxide occurs as Co_3O_4 in the initial state and the ultimate reduction state is Co^0.

For chemisorption study, a standard pretreatment of the catalyst samples was adopted which involves outgassing at room temperature for 2 h then heating at 330 °C for 1 h at $p \sim 10^{-5}$ torr (1 torr = 1.333 × 10^2 Pa). The adsorption isotherm of pure H_2 was determined at 330 °C in the pressure range up to ~ 200 torr (1st isotherm) in a conventional volumetric apparatus [26]. The catalyst sample was outgassed for 1 h at 330 °C and the second isotherm was measured in the same manner.

The degree of dispersion of supported cobalt, [H]/[Co], was calculated from the net adsorption uptakes of H_2, taking into consideration the fraction of cobalt reduced, α, [26, 27]. The specific surface area of supported cobalt could be calculated according to [26]

$$S_{Co} = \frac{N\sigma}{A_k}\frac{[H]}{[Co]} \quad (2)$$

where N is Avogadro's number, A_k is atomic weight of cobalt and σ is the cross-sectional area of cobalt atom, taken as 6.25×10^{-20} m^2 [26].

From XRD observation that supported cobalt exists mainly as fcc crystallites, the average particle size (d_{Co}, nm) could be determined as based on the first approximation that all Co crystallites are ideal cubes of uniform size with one face in contact with the support surface and the remaining five faces exposed [26, 27], hence

$$S_{Co} = \frac{5}{\rho_{Co}\, d_{Co}} \quad (3)$$

where ρ_{Co} is the particle density of cobalt taken as 8.86 g cm^{-3} [28, 29].

2.6. BET surface area and pore analysis

Adsorption–desorption isotherms of pure N_2 gas were measured at 77 K using a conventional volumetric apparatus. Specific surface areas were calculated from the isotherms by applying the BET equation [30]. The porosity of the samples was detected by means of V_1–t plots [31, 32].

2.7. X-ray diffraction analysis

The analysis was performed using a Philips P.W. 1050/25 diffractometer and P.W. 1965/40 goniometer

with iron filtered cobalt radiation at 40 kV and 30 mA. The scanning speed of line broadening was 1/8°, 10 mm min^{-1}.

2.8. Infrared analysis

A Pye–Unicam infrared spectrophotometer, model SP 3-200, was used adopting the KBr technique.

2.9. Thermogravimetric analysis

Thermogravimetric analysis (TGA) of different catalyst samples was carried out in the presence of static air at heating rate of 10° C min^{-1} using a Stanton–Redcroft thermobalance type 750/770 connected to a Kipp and Zonnen BD9 two-channel automatic recorder.

3. Results and discussion

3.1. Physicochemical characteristics of the studied catalyst samples

The XRD pattern of the unsupported cobalt oxide treated under the same preparational conditions of the supported catalysts were those characteristic of Co_3O_4 of fcc shape (d = 0.467, 0.286, 0.244, 0.156, and 0.143 nm). For pure titania support, the obtained bands corresponded to the anatase form of tetragonal shape (d = 0.352, 0.238, 0.189, 0.170, 0.167, 0.148, and 0.126 nm). All the supported samples, undoped and V_2O_5-doped, showed mainly the bands of TiO_2 support with an additional diffraction line at d = 0.244 nm, which is the most intense band of Co_3O_4 phase. The characteristic bands of V_2O_5 could not be observed in doped samples. No phase transformation was noticed either for Co_3O_4 or TiO_2 phases upon heat treatment up to 600 °C.

From infrared spectral analysis, complete decomposition of the cobalt nitrate into the respective oxide was found to occur only at $t \geqslant 330$ °C, which revealed the proper choice of this temperature, i.e. 330 °C, as a starting calcination temperature in the present study.

TGA showed that the physisorbed water was lost in the temperature range up to ~ 200 °C after which no loss in weight was observed up to 700 °C. Both differential thermal analysis (DTA) and TGA confirmed that neither phase transformation nor dehydroxylation takes place within the temperature range 200–700 °C.

3.2. Catalytic activity of thermally treated samples

The activity of various samples of the undoped and V_2O_5-doped Co_3O_4/TiO_2 catalysts, measured in H_2O_2 decomposition, was expressed in terms of A/A_0, where A is the activity of the catalyst treated for a given time at a given temperature, and A_0 is the activity of the freshly prepared catalyst [21]. Fig. 1 illustrates this activity as a function of time, temperature and atmosphere of thermal treatment. The effect of thermal treatment on the activity is widely different in the two catalyst systems. For the undoped catalyst,

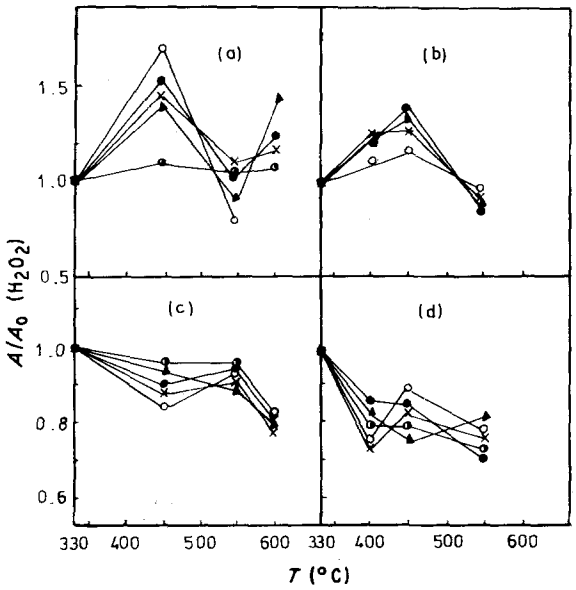

Figure 1 Relative activity $(A/A_0)_{H_2O_2}$ of various samples of (a, b) undoped Co_3O_4/TiO_2 catalyst and (c, d) V_2O_5-doped Co_3O_4/TiO_2 catalyst, as a function of time, temperature and thermal treatment atmosphere. Time: (○) ½, (×) 1, (▲) 2, (●) 4, (◑) 6 h; (a, c) in air, (b, d) in vacuum.

the maximum activity in both studied atmospheres, vacuum and air, is achieved at 450 °C. This activation temperature was recorded previously for some unsupported oxides, e.g. [33], as well as for several metallic supported catalysts [21, 26, 34]. The observed activation process may be attributed to the fact that at 450 °C (close to Tamman's temperature), the migration of defects on the titania surface becomes rapid enough [35] for it to retard the association of the surface-active particles. On the other hand, the deactivation isotherms of both the unsupported Co_3O_4 and the supported Co_3O_4/TiO_2 catalysts obtained at 550 °C in air (Fig. 2) were analysed according to the previously published method [34]. The analysis showed that the deactivation of Co_3O_4 follows a second-order mechanism, whereas in the case of the supported catalyst, it follows an unrealistic high order (~ 19). The second-order mechanism can be interpreted along the same lines as reported elsewhere [21, 26, 34], whereas the high-order mechanism seems to be linked with the pore system, the metal dispersion and the nature of the controlling reaction [34].

For the V_2O_5-doped catalyst, a slight gradual deactivation takes place in the two studied pretreatment atmospheres (Fig. 1). In general, the V_2O_5 dopant seems to affect the migration of defects on the TiO_2 surface and the mode of dispersion of cobalt active particles. The pronounced deactivation at high temperatures indicates most probably the strong interaction between the supported phases and the TiO_2 support.

The activation parameters of the test H_2O_2 decomposition reaction, being known to be effectively dependent on the catalyst nature rather than its morphology [36], were tested through the so-called "compensation effect" [37, 38]. This effect involves the correlation

$$\log Z_0 = B + eE \qquad (4)$$

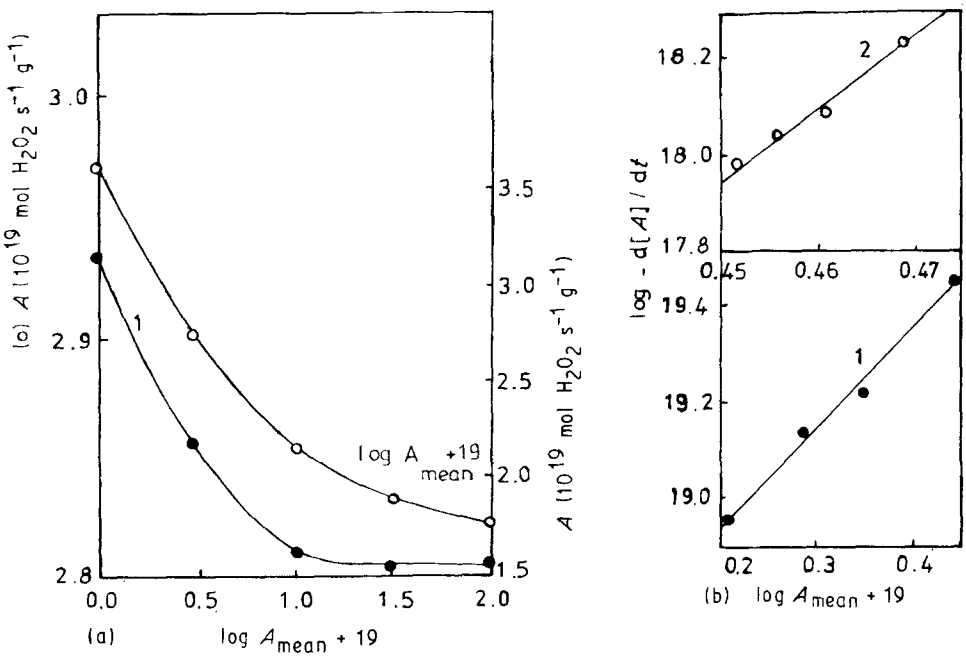

Figure 2 (a) Air-sintering isotherms at 550 °C for: 1, unsupported Co_3O_4; 2, supported Co_3O_4/TiO_2 catalyst. (b) Differential treatment of the sintering isotherms.

where Z_0 is the Arrhenius pre-exponential factor, taken as a measure of the density of active sites, E is the activation energy of the reaction, B and e are constants and $1/e = 2.303\,R\beta$ (β is known as the isokinetic temperature [37]. The obtained results under widely different conditions, i.e. chemical nature of the catalyst, time, temperature and atmosphere of heat treatment, are illustrated in Fig. 3, revealing the same kinetic pattern in all cases and producing the same values of B and e, namely 6.31 and 6.6×10^{-4}, respectively. The calculated value of e corresponds to 329 K, which lies very closely within the temperature range of the kinetic experiments of the test reaction, but does not reflect any of the pretreatment temperatures in contrast to that earlier reported by several investigators, e.g. [37, 39–41]. The results suggest that the reaction mechanism, under the studied variables, is almost the same and the step of oxygen diffusion (and/or desorption) is the rate limiting one, because it is the only reaction factor being subject to changes when the other prescribed factors are altered [20]. The compensation effect may also assume a continuous redistribution of active centres of various energy states during the heat treatment; the involvement of Co^{II}/Co^{III} as a highly active equilibrium couple is a prime requirement for the catalyst systems studied under the present conditions [20, 33].

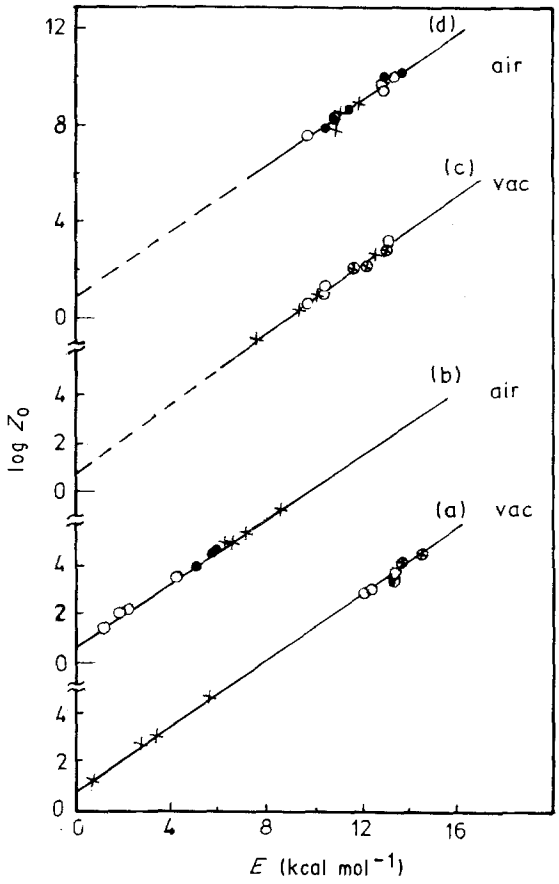

Figure 3 Compensation parameters for the H_2O_2 decomposition reaction over (a, b) supported Co_3O_4/TiO_2 catalyst and (c, d) V_2O_5-doped Co_3O_4/TiO_2 catalyst. (●) 400 °C, (×) 450 °C, (○) 550 °C, (⊗) 600 °C.

3.3. Active species as estimated from dissolution and excess oxygen data

The fraction of free Co_3O_4 that could be extracted under the above conditions is given in Table I, as normalized to 1 g of the supported oxide ($X_f^{Co_3O_4}$). It is evident, for the freshly prepared catalyst, that only about 9% of the supported oxide exists as free Co_3O_4 whereas the major fraction is combined with the support. This combined fraction may be assigned to both Co-o and Co-t resulted from diffusion of cobalt ions into the octahedral and tetrahedral sites of the titania support, respectively [4, 6]. Other phases may also be formed [15]. The V_2O_5 dopant does not seem to have a considerable effect on the fraction of free Co_3O_4. The obtained results for the undoped catalyst treated for 2 h are in good harmony with the activity

TABLE I Total number of Co^{3+} ions and specific activity, [a], as estimated from active oxygen measurements, and distribution of various cobalt species in freshly prepared and thermally treated catalyst samples for 2 h

T (°C)	$[Co^{3+}]_{tot}$ (10^{19})	[a] $\left(\frac{\text{molec. } H_2O_2}{\text{s } Co^{3+}\text{ ion}}\right)$	α ($= X_R^{Co}$)[a]	$X_f^{Co_3O_4}$[b]	X_R^{Co-o}[c]	X_N^{Co-t}[c]
Co_3O_4/TiO_2 (F.P.)						
	3.72	12	0.54	0.09	0.45	0.46
Vac-treatment						
450	5.35	11	0.55	0.18	0.37	0.45
550	4.83	10	0.49	0.11	0.38	0.51
600	4.50	10	0.50	0.03	0.47	0.50
Air-treatment						
400	5.63	10	0.67	0.10	0.57	0.33
450	5.10	11	0.60	0.10	0.50	0.40
550	4.20	10	0.50	0.06	0.44	0.50
		av. = 10				
V_2O_5–Co_3O_4/TiO_2 (F.P.)						
	6.05	9	0.87	0.08	0.79	0.13
Vac-treatment						
450	4.48	10	0.73	0.14	0.59	0.27
550	3.95	11	0.67	0.03	0.64	0.33
600	3.15	10	0.50	0.02	0.48	0.50
Air-treatment						
400	6.00	11	0.71	0.11	0.60	0.29
450	4.06	10	0.69	0.12	0.57	0.31
550	3.70	10	0.58	0.09	0.49	0.42
		av. = 10				

[a] All parameters are calculated as fractions of cobalt by weight.
[b] From dissolution data.
[c] R, reducible species; N, non-reducible species.

data (Fig. 1). The increase, obtained at 450 °C, in the free fraction of the oxide may be attributed to the mobilization of active particles from deeper layers to the outer ones [6, 7, 15]. For the doped catalyst, the obtained results differ greatly from the activity data. During vacuum-treatment at $t > 450$ °C, the dopant seems to enhance the interaction of active cobalt species with the support, whereas in atmospheric air, the fraction of free oxide increases relatively with some stabilization over the whole temperature range studied; the effect has been reported previously for some other systems [6, 7].

The results of surface and bulk excess oxygen, corrected and expressed in terms of at % $g^{-1}_{Co_3O_4}$, are shown in Fig. 4 after 2 h treatment. The surface excess oxygen decreases continuously with increasing temperature in all cases, which may be connected with the rate of oxygen desorption in both atmospheres [35]. The bulk excess oxygen, however, changes in a similar manner to that of the activity (cf. Fig. 1). This is well documented in Table I (columns 2 and 3) in terms of the constancy of the specific activity, i.e. $a = [A]/Co^{3+}_{tot}$; the average activity being 10 molec. H_2O_2 (s ion $Co^{3+})^{-1}$ (the total number of Co^{3+} ions was calculated per g supported Co_3O_4 as mentioned above). This result indicates the importance of Co^{3+} ions as active sites, or more probably the Co^{II}/Co^{III} couples, and their involvement in the rate-determining step. It may, thus, provide additional evidence for the obtained compensation effect, assuming Z_0 to represent the concentration of cationic vacancies or that of

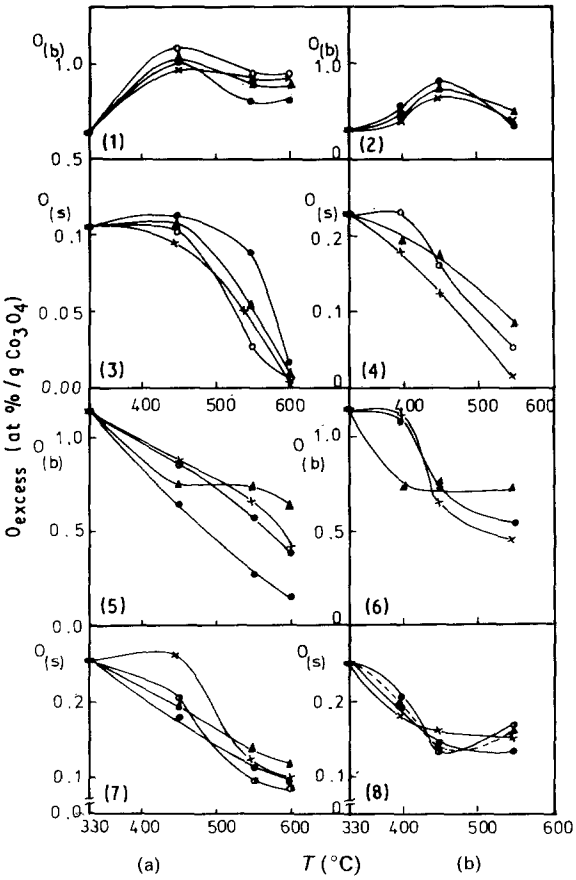

Figure 4 Surface excess oxygen, $O_{(s)}$, and bulk excess oxygen, $O_{(b)}$, as a function of time, temperature and atmosphere of thermal treatment of (1–4) undoped and (5–8) doped Co_3O_4/TiO_2 catalysts. Time: (○) ½, (×) 1, (▲) 2, (●) 4, (◑) 6 h; in (a) vacuum, (b) air.

Co^{3+} centres of various activation energies. The production of the bulk Co^{3+} ions may take place at the expense of some surface well-dispersed Co^{2+} ions and some Co_3O_4 crystallites penetrating into the subsurface layer of the titania support [4]. Some Ti^{4+} may also be forced to diffuse to the surface [15]. The migration of oxygen species (mainly as O^- and O^{2-}), being increased by thermal treatment, may push the lattice oxygen ahead towards the vacancy or defect where Co^{2+} is located leading to its conversion to Co^{3+} [42].

3.4. Reducibility and distribution of various cobalt species

The degree of reducibility, α, is by itself a measure of the fraction of the reducible phases of cobalt in the catalyst systems studied, i.e. X_R^{Co}. The readily reducible phases include both the surface-free bulk-like Co_3O_4 ($X_f^{Co_3O_4}$) estimated from dissolution data and the Co^{2+} species occupying the weaker octahedral sites of the TiO_2 support, X_R^{Co-o} [4, 6, 7]. The remaining fraction of non-reducible cobalt may represent the subsurface cobalt species interacting strongly with tetrahedral sites of TiO_2, i.e. X_N^{Co-t} [15].

From the parallelism between the reducibility and the activity data of different catalyst samples treated for 2 h at different temperatures and in different atmospheres (Table I, column 4 and Fig. 1), it may be assumed that the active species are thus the easily reducible ones. The surface-free species seem to be more important. The non-reducible fraction, (Co-t), however, shows a general increase with increasing temperature. At higher temperatures, this fraction appears to take place mostly at the expense of the surface-free species (Table I, columns 5, 6 and 7).

Of special interest is the effect of doping, where the degrees of reducibility of freshly prepared and various thermally treated samples are higher than the corresponding ones of the undoped samples. For the freshly prepared catalyst, as no marked effect is shown in the fraction of surface-free species, the fraction of Co-o seems to undergo a considerable increase. This favours the idea that vanadium diffuses a few atomic layers deeper into the titania support occupying most of the near subsurface tetrahedral sites and thus leading to the repositioning of cobalt into weaker octahedral sites. The possibility of interaction between vanadium and cobalt, which renders the cobalt more reducible and therefore inhibits the formation of more free Co_3O_4 phase cannot be excluded [43]. As the temperature increases, the tetrahedral sites become gradually more available for occupation by cobalt.

Although other phases may exist, the assumptions given here are limited to the interacting species, Co-o and Co-t, just to model their behaviour upon doping and during heat treatments.

3.5. Degree of dispersion and average particle size

Because the cobalt crystallite size in the catalysts under study is too small to be measured by XRD techniques, it seems that chemisorption is the only approach to measure the metal dispersion.

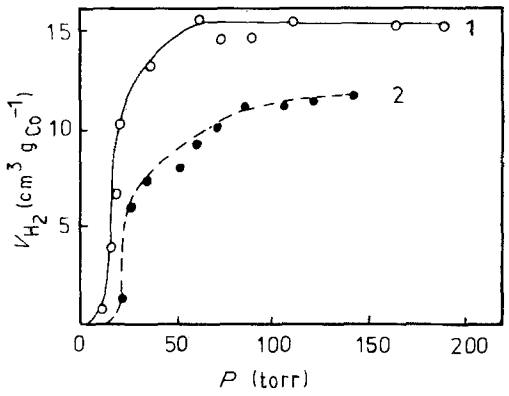

Figure 5 H_2 adsorption isotherms at 330 °C on reduced freshly prepared Co_3O_4/TiO_2 catalyst.

The high-temperature chemisorption of H_2 was followed according to the above technique. Typical first (adsorption) and second (resorption) isotherms on the reduced undoped Co_3O_4/TiO_2 catalyst are shown in Fig. 5. Similar isotherms were obtained for the doped and thermally treated samples. The net adsorption on the supported cobalt was calculated from the difference between the first and the second isotherms taking into consideration the degree of reducibility. The results of H_2 chemisorption on freshly prepared catalysts, as well as on various samples treated for 2 h at different temperatures in different atmospheres, are summarized in Table II. The degree of dispersion of supported cobalt, [H]/[Co], in the undoped catalyst samples is shown to change with temperature in a similar manner to that of the activity (Fig. 1). Higher degrees of dispersion are accompanied by a decrease in particle size (d_{Co}) and a corresponding increase in the metallic surface area (S_{Co}). The minimum dispersion which occurred at 550 °C in air is characterized

TABLE II Hydrogen-adsorption data on the reduced freshly prepared catalysts and various samples treated for 2 h at different temperatures in different atmospheres

T (°C)	$(H_2)_{net\ ads.}$ (mmol g_{Co}^{-1})	[H]/[Co]	d_{Co} (nm)	S_{Co} ($m^2\ g^{-1}$)
Freshly prepared Co_3O_4/TiO_2	0.31	0.092	9.6	58.8
Vac-treatment				
450	0.47	0.138	6.4	88.1
550	0.42	0.137	6.5	87.5
600	0.40	0.130	6.8	83.0
Air-treatment				
400	0.80	0.177	5.0	113.0
450	0.74	0.160	5.5	102.0
550	0.13	0.043	20.5	27.0
Freshly prepared V_2O_5–Co_3O_4/TiO_2	2.27	0.420	2.1	268.2
Vac-treatment				
450	0.67	0.145	6.1	92.6
550	0.80	0.192	4.6	122.6
600	0.97	0.210	4.2	134.1
Air-treatment				
400	1.25	0.282	3.1	158.3
450	0.72	0.125	6.1	94.0
550	0.58	0.118	8.2	69.2

TABLE III Nitrogen-adsorption data and pore structure characteristics of pure Co_3O_4, TiO_2 support, freshly prepared catalysts and various samples treated for 2 h at different temperatures in different atmospheres

T (°C)	BET-C constant	S_{BET} ($m^2 g^{-1}$)	V_p ($ml g^{-1}$)	S_t ($m^2 g^{-1}$)	S^{cp}_{cum} ($m^2 g^{-1}$)	V^{cp}_{cum} ($ml g^{-1}$)	S_n/S^{cp}_{cum}
Pure Co_3O_4	4	113.2	0.132	107.5	113.0	0.125	0.27
Orig. TiO_2	5	98.9	0.115	92.0	98.7	0.110	0.24
Soaked TiO_2	8	71.2	0.125	85.0	88.0	0.129	0.24
Freshly prepared							
Co_3O_4/TiO_2	4	111.3	0.129	106.0	111.2	0.137	0.27
Vac-treatment							
450	4	104.6	0.118	100.0	102.2	0.118	0.25
550	4	110.5	0.113	98.5	118.0	0.103	0.26
600	4	111.3	0.131	103.0	109.3	0.118	0.24
Air treatment							
400	4	113.1	0.106	106.0	108.0	0.092	0.33
450	4	92.7	0.076	78.0	114.0	0.075	0.30
550	5	77.1	0.085	74.0	73.7	0.072	0.26
Freshly prepared							
V_2O_5–Co_3O_4/TiO_2	4	123.5	0.244	130.0	118.0	0.247	0.20
Vac-treatment							
450	4	207.5	0.722	206.0	197.5	0.692	0.10
550	4	192.5	0.786	195.0	201.7	0.766	0.09
Air-treatment							
400	4	107.0	0.276	115.0	106.5	0.242	—
450	6	117.1	0.699	130.0	130.0	0.687	—
550	3	185.2	0.890	162.0	182.0	0.775	—

by an enlargement in particle size from 9.6 to 20.5 nm with a considerable reduction in metallic surface area, i.e. to ~ 50%.

Upon doping with V_2O_5, the degree of dispersion shows a marked increase indicating the importance of particle size effect in addition to the possible detachment of some Co-t species. The large decrease in particle size (from 9.6 to 2.1 nm) may favour the substitution mechanism of some Co^{2+} or Co^{4+} by V^{5+} or V^{4+} ions (radii of Co^{2+} = 0.078 nm, Co^{3+} = 0.056 nm; average = 0.067 nm, and V^{5+} = 0.040 nm, V^{4+} = 0.061 nm; average = 0.061 nm [28]). This may be accompanied by a shrinkage in the lattice parameters leading, thereby, to smaller mobile particles which develop much higher metallic surface areas, the trend being common for various doped samples and may be linked with the ease of reducibility.

3.6. Surface texture of the investigated catalyst samples

Typical adsorption–desorption isotherms of N_2 on the surface of some selected samples, namely original and soaked titania (the soaked sample was that treated under the same pH, drying and calcination conditions applied for the preparation of parent catalysts), freshly prepared catalysts and samples treated thermally for 2 h at 450 °C *in vacuo* and in air, are shown in Fig. 6. All isotherms seem to belong to type II of Brunauer and Emmett's classification [44] which are completely reversible on the support samples. For the different catalyst samples, closed hysteresis loops are exhibited which undergo some modification upon doping.

The adsorption data for all samples under study are summarized in Table III, including BET-C constants and specific surface areas (S_{BET}) calculated by applying the BET equation and total pore volumes (V_p) estimated from the saturation values of the adsorption isotherms. The results of the freshly prepared supported catalyst are very close to those of the unsupported Co_3O_4 reflecting, most probably, the

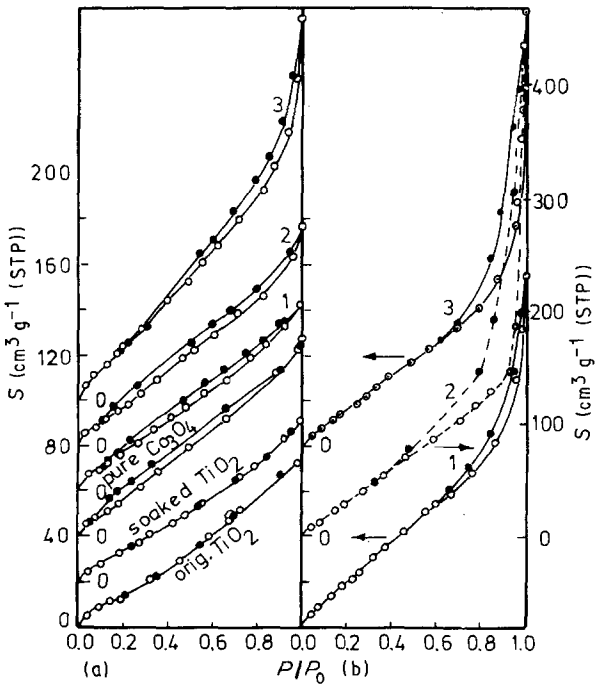

Figure 6 Typical adsorption–desorption isotherms of N_2 on the surface of (a) undoped Co_3O_4/TiO_2 catalyst; 1, freshly prepared; 2, treated for 2 h at 450 °C *in vacuo*; 3, treated for 2 h at 450 °C in air; (b) V_2O_5-doped catalyst; 1, freshly prepared; 2, treated for 2 h *in vacuo*; 3, treated for 2 h in air (reversible isotherms on titania support are also shown).

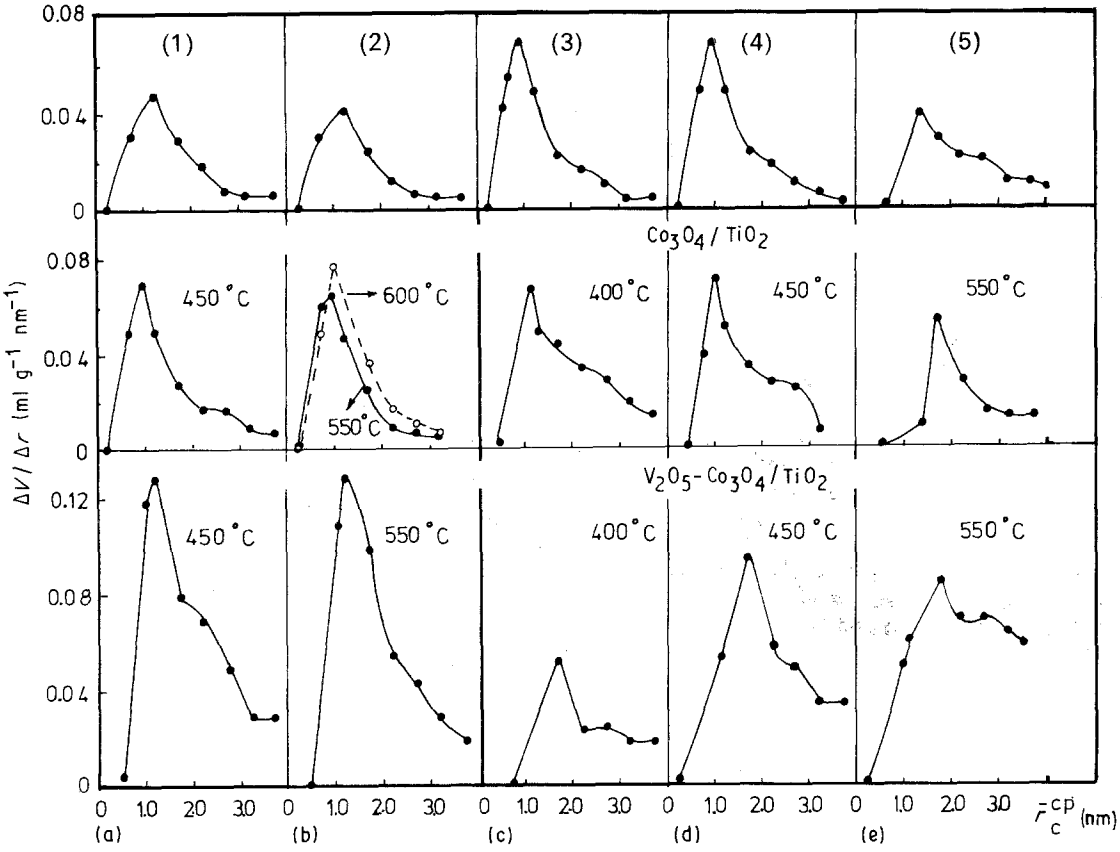

Figure 7 Pore size distribution curves for (1) original TiO_2, (2) soaked TiO_2, (3) pure Co_3O_4, (4) freshly prepared Co_3O_4/TiO_2 catalyst, (5) freshly prepared V_2O_5–Co_3O_4/TiO_2 catalyst and various samples treated for 2 h at different temperatures in different atmospheres. (a, b) vacuum treatment, (c–e) air treatment.

monolayer coverage of the titania support by cobalt oxide phase. Doping with V_2O_5 seems to develop a new pore system with higher adsorption parameters.

For pore structure analysis, reference t-curves were constructed by several investigators based on the adsorption of N_2 on non-porous solids. The appropriate t-curves were chosen according to the BET-C constants, which in each case should be of the same order in both the reference t-curve and the catalyst under investigation. The t-curve of Mikhail *et al.* [45], characterizing non-porous solids with low BET-C constants (< 30) was used for all samples in the present study. V_l–t plots were constructed, where V_l is the volume of N_2 adsorbed (ml g^{-1}) and t is the statistical thickness (nm). From the slope of the straight line obtained passing through the origin, the specific surface area, S_t, was calculated. The reasonable agreement between S_{BET} and S_t is the main criterion for the correct choice of the t-curve used in the analysis (Table III).

The obtained V_l–t plots indicated that all samples under investigation are predominantly mesoporous. The analysis of these pores was carried out using the corrected modelless method [46] assuming a cylindrical pore model (cp) and the resultant cumulative parameters, S_{cum}^{cp} and V_{cum}^{cp}, are given in Table III. A trial was also made to estimate the surface evolved from the fraction of micropores, S_n, being analysed according to the MP method [45]. It is clear from the S_n/S_{cum}^{cp} ratio that, in the case of the undoped catalyst, the atmospheric air reflects a more pronounced effect on the microporosity characteristics. Doping with V_2O_5 could lead to a decrease in the surface area located in micropores which continues to disappear rapidly upon thermal treatment.

The pore volume distribution curves shown in Fig. 7, representing the distribution of pore volumes ($\Delta V/\Delta r$) as a function of the mean core radii ($\bar{r}_c^{cp}$, nm), support the above findings. For soaked titania, a little increase in the pore width occurs compared with the original titania, i.e. $\bar{r}_c^{cp}$ changes from 1.2 to 1.25 nm having no effect on the microporosity. For the freshly prepared unsupported Co_3O_4 and supported Co_3O_4/TiO_2 catalysts, the distribution curves are very similar, $\bar{r}_c^{cp}$ being 1.0 nm for both, with the contribution of the same fraction of micropores. Vacuum treatment has little effect, whereas air treatment leads to some increase in the narrow fraction of pores. Doping with V_2O_5 shows little widening effect ($\bar{r}_c^{cp} =$ 1.4 nm). While vacuum treatment is associated with a gradual increase in the population of the narrow-ranged mesopores, air treatment seems to be associated with a gradual shift towards larger most frequent core radii. This may reflect the role of the dopant and its diffusion in modifying the porosity characteristics of the titania support.

In conclusion, it is evident that doping with V_2O_5 could affect both surface and bulk diffusion of active cobalt oxide particles upon thermal treatment of the supported Co_3O_4/TiO_2 catalyst under investigation. The dopant seems to have a two-fold effect: part is incorporated into surface Co_3O_4 crystallites leading to smaller more mobile particles, easily reducible and more dispersed, and another part is diffused into the

support, leading to redistribution of various cobalt species, namely Co-t and Co-o. The bulk diffusion enhanced by doping may cause, upon heating, some modification in the porosity characteristics of the titania support.

References

1. M. F. L. JOHNSON and H. E. RIES Jr, *J. Phys. Chem.* **57** (1953) 865.
2. P. GAJARDO, P. GRANGE and B. DELMON, *ibid.* **83** (1979) 1771.
3. P. GAJARDO, D. PIROTTE, P. GRANGE and B. DELMON, *ibid.* **83** (1979) 1780.
4. K. S. CHUNG and F. E. MASSOTH, *J. Catal.* **64** (1980) 320.
5. M. HOUALLA and B. DELMON, *Appl. Catal.* **1** (1981) 285.
6. R. L. CHIN and D. M. HERCULES, *J. Phys. Chem.* **86** (1982) 360.
7. *Idem, J. Catal.* **74** (1982) 121.
8. S. J. TAUSTER and S. C. FUNG, *ibid.* **55** (1978) 29.
9. P. KOFSTAD, *J. Less-Common Metals* **13** (1974) 635.
10. T. IWAKI, M. KOMURO and K. HIROSAWA, *J. Catal.* **39** (1975) 324.
11. S. J. TAUSTER, S. C. FUNG, R. T. BAKER and J. A. HORSLEY, *Science* **211** (1981) 1121.
12. J. A. HORSLEY, *J. Amer. Chem. Soc.* **101** (1979) 2870.
13. B. A. SEXTON, A. E. HUGHES and K. FOGER, *J. Catal.* **77** (1982) 85.
14. G. T. POTT and W. H. J. STOCK, in "Preparation of Catalysts", edited by B. Delmon, P. A. Jacobs and G. Poncelet (Elsevier Scientific, Amsterdam, 1976) p. 537.
15. P. ARNOLDY and J. A. MOULIJN, *J. Catal.* **93** (1985) 38.
16. P. C. GRAVELLE, G. EL-SHOBAKY and S. J. TEICHNER, in "Proccedings of the Symposium on Electronic Phenomena in Chemical Catalysis by Semiconductors", edited by K. Hauffe and Th. Volkenstein (Moscow, 1968) p. 124.
17. G. EL-SHOBAKY, N. M. GHONEIM, I. F. HEWAIDY and I. M. MORSI, *Thermochim. Acta* **61** (1983) 107, and other references therein.
18. P. KOSTAD, "Non-Stoichiometry, Diffusion and Electrical conductivity in Binary Metal Oxides" (Wiley-Interscience, New York, 1972) p.426.
19. A. LYCOURGHIOTIS, A. TSIATSIOS and N. KATSANOS, *Z. Phys. Chem.* **126** (1981) 85.
20. J. R. GOLDSTEIN and A. A. TSEUNG, *J. Catal.* **32** (1974) 452.
21. S. A. HASSAN, F. H. KHALIL and F. G. EL-GAMAL, *ibid.* **44** (1976) 5.
22. S. W. WELLER and S. E. VOLTZ, *J. Amer. Chem. Soc.* **76** (1954) 4695.
23. A. BIELANSKI, J. DEREN, J. HABER and J. SLOCZYNSKI, *Trans. Faraday Soc.* **58** (1962) 166.
24. R. B. ARORA, R. K. BANERJEE, N. K. MANDOL, N. C. GANGULI and S. P. SEN, *Technology (Sindri, India)* **8** (1971) 107.
25. J. A. AMELSE, L. H. SCHWARTZ and J. B. BUTT, *J. Catal.* **72** (1981) 95.
26. S. A. HASSAN, M. ABDEL-KHALIK and H. A. HASSAN, *ibid.* **52** (1978) 261.
27. R. C. REUEL and C. H. BARTHOLOMEW, *ibid.* **85** (1984) 63.
28. V. A. ROITER, "Catalytic Properties of Materials", Handbook (Naukova Dumka, Akad. Nauk, Keiv, USSR, 1968) p. 721.
29. A. A. TSEUNG and J. R. GOLDSTEIN, *J. Mater. Sci.* **7** (1972) 1383.
30. S. BRUNAUER, P. H. EMMETT and E. TELLER, *J. Amer. Chem. Soc.* **60** (1938) 309.
31. B. C. LIPPENS, B. G. LINSEN and J. H. DE BOER, *J. Catal.* **3** (1964) 32.
32. J. H. DE BOER, B. G. LINSEN and Th.J. OSINGA, *ibid.* **4** (1965) 643.
33. J. DEREN, J. HABER, A. PODGORECKA and J. BURZYK, *ibid.* **2** (1963) 161.
34. S. A. HASSAN, G. I. EMEL'YANOVA, V. P. LEBEDEV and N. I. KOBOZEV *Zh. Fiz. Khim.* **44** (1971) 1469.
35. J. HABER, in "Advances in Catalysis", Vol. 29, edited by J. R. Anderson, and M. Boudart, (Springer-Verlag, Berlin, Heidelberg, (1981) Ch. II, p. 87.
36. W. C. SCHUMB, C. N. SATTERFIELD and R. L. WENTWORTH, "Hydrogen Peroxide" (Reinhold, New York 1955) Ch. 8, pp. 472–476.
37. K. GOZNER and H. BISCHOF, *J. Catal.* **32** (1974) 175.
38. D. D. ELEY, H. PINES and P. B. WEISZ, in "Advances in Catalysis", Vol. 26, edited by A. K. Galway (Academic Press, New York, London, 1977) p. 247).
39. G. M. SCHWAB and E. GREWER, *Z. Phys. Chem.* **A144** (1929) 243.
40. *Idem, ibid.* **B5** (1929) 406.
41. G. M. SCHWAB, *Adv. Catal.* **2** (1950) 251.
42. V. A. SHVETS and J. H. KAZANSKY, *J. Catal.* **25** (1972) 123.
43. F. A. KROGER, "Chemistry of Imperfect Crystals" (North-Holland, Amsterdam, 1964).
44. S. BRUNAUER and P. H. EMMETT, *J. Amer. Chem. Soc.* **57** (1935) 1745.
45. R. Sh. MIKHAIL, S. BRUNAUER and E. E. BODOR, *J. Colloid. Interface Sci.* **26** (1968) 45.
46. S. BRUNAUER, R. Sh. MIKHAIL and E. E. BODOR, *ibid.* 24 (1967) 451.

Received 11 September 1989
and accepted 7 March 1990